SUPPLEMENTARY MATERIAL

Supplementary Figure Legends

Supplementary Figure S1.

Overexpression of mVENUS-Sec22bΔTMD or mVENUS-VAMP3ΔTMD inhibits phagocytosis in J774 macrophages.

(A) Green signals indicate mVENUS-tagged proteins stably expressed in J774 cells. The signals of mVENUS and mVENUS-Sec22bΔTMD were distributed throughout the cells, but overexpression of VAMP3ΔTMD produced some dot-like structures, as shown in the inset. *Bars*, 20 μm. (B) Western blotting analysis of total lysates from J774 cells stably expressing mVENUS, mVENUS-Sec22bΔTMD, and mVENUS-VAMP3ΔTMD. Western blotting was carried out using antibodies against EGFP, Sec22B, and VAMP3. Asterisks (*) denote non-specific band recognized by anti-VAMP3 antibodies (Affinity BioReagents, Inc., Golden, CO). (C) J774/mVENUS, J774/mVENU-Sec22bΔTMD, and J774/mVENUS-VAMP3ΔTMD cells were incubated with luminol-bound microbeads. Chemiluminescence from cells that ingested the beads was measured on a TD-20/20 luminometer for 15 sec every 1 min at a 50.1% sensitivity level. The results are given in relative light units (RLUs). These results were normalized to the maximal value obtained for J774/mVENUS cells within the same experiment. Data presented are the mean ± S.E. of three independent experiments.

Supplementary Figure S2.

Fraction of phagosomes labeled with LAMP-1 antibodies and with mVENUS-syntaxin 18.

(A) J774/mVENUS-syntaxin 18 cells were incubated with non-opsonized latex beads (3.0-μm diameter) for 10, 20, 40, or 120 min. The cells were fixed with 4% paraformaldehyde for 20 min

at room temperature and permeabilized with 0.2% Triton X-100 for 30 min. Then the cells were stained with an anti-LAMP-1 antibody in combination with Alexa594-labeled secondary antibodies. Asterisks (*) denote phagosomes in the cells that contain a latex bead. Phagosomes labeled with mVENUS-syntaxin 18 were classified into three types. Type-1 and type-3 indicate LAMP-1–negative and –positive phagosomes, respectively. Type-2 shows a phagosome partially detected by LAMP-1 signals. (B) Quantitation of each type of phagosome over time. Values are expressed as a percent of the total number of the three types of phagosomes (fifty phagosomes) at the indicated time points. Data presented are the mean ± S.E. of three independent experiments. The rate of LAMP-1–positive phagosomes gradually increased within the first 40 min. This is consistent with the results in Figure 1 using J774 cells, suggesting that J774/mVENUS-syntaxin 18 cells have retained the normal phagocytic function of J774 cells.

Supplementary Figure S3.

Electron micrographs of purified phagosomes and 0.8-μm-diameter beads used for phagocytosis.

(A) Additional electron micrographs of purified phagosomes from the J774/mVENUS-syntaxin 18 cells described in Figure 7. We observed a mean of 9.8 ±1.4 gold particles on each phagosome (n = 20) whose major axis is in the 720 to 900 nm range. (B) In contrast, no significant gold signal was detected on phagosomes from J774 cells (n = 50). (C) The electron microscopic experiment was performed on 0.8-μm-diameter beads alone as a control. No structure was detected on the bead, suggesting that visible structures surrounding the bead in (A) and (B) are truly phagosomal membranes. *Bars*, 200 nm.

Supplementary Figure S4.

No difference was observed in the shape and size of J774 cells expressing mVENUS and mVENUS-syntaxin 18.

Green signals indicate mVENUS-tagged proteins expressed in J774 cells. Differential interference contrast (DIC) images indicate the cell shape and size. *Bars*, 10 μm.

Supplementary Figure S5.

J774/mVENUS-syntaxin 18 cells enhance the rate of phagocytosis in a Texas Red–conjugated zymosan A (*S. cerevisiae*) assay. J774/mVENUS and J774/mVENUS-syntaxin 18 cells were incubated with Texas Red–conjugated zymosan particles for the indicated times in the presence (+) and absence (-) of cytochalasin B (final concentration 10 μM). The cells were washed thoroughly with PBS to remove free particles and fixed. Quantitation of each image is summarized in Figure 7E. *Bar*, 20 μm.

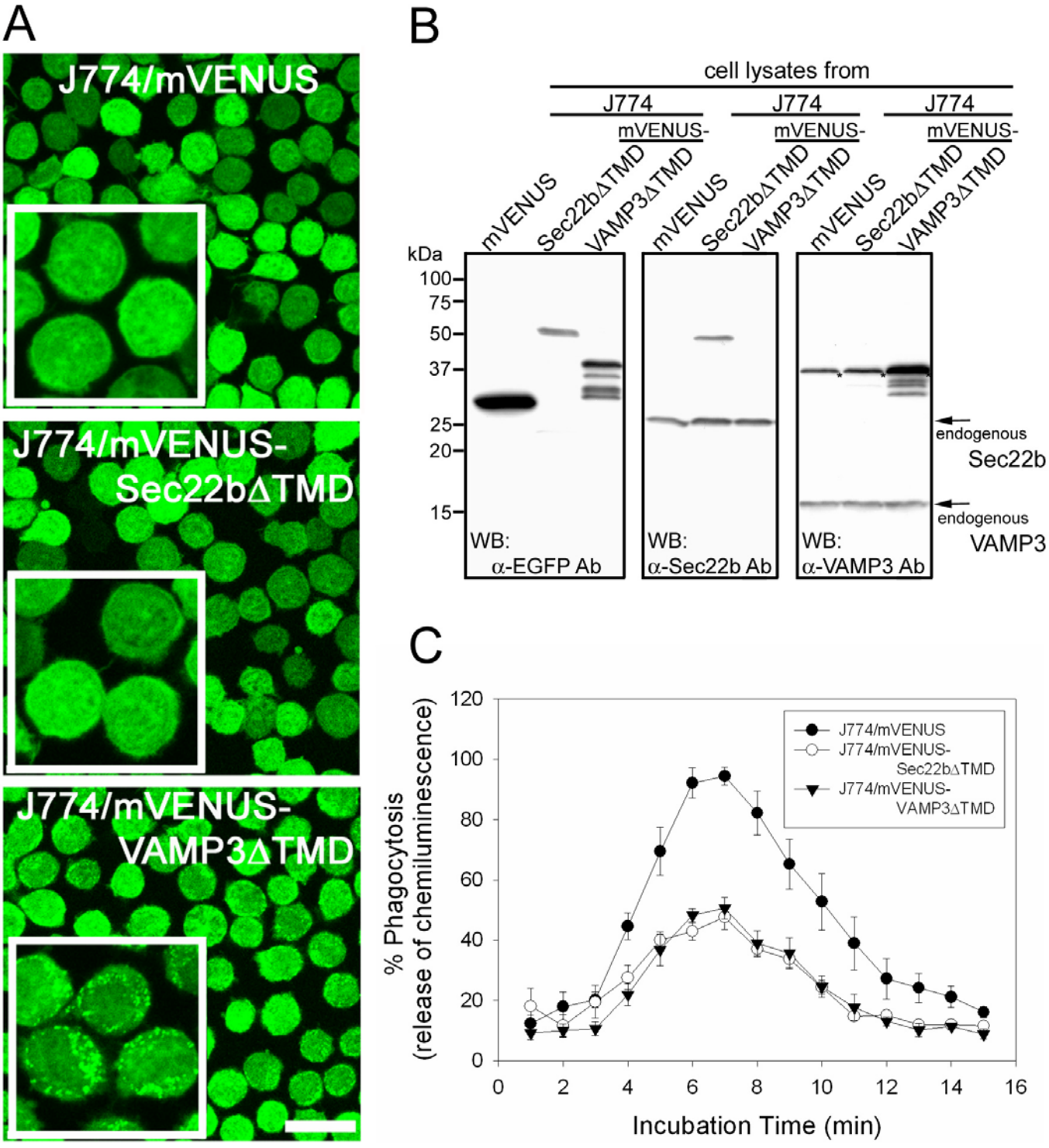

Supplementary Figure S1. Hatsuzawa *et al.*

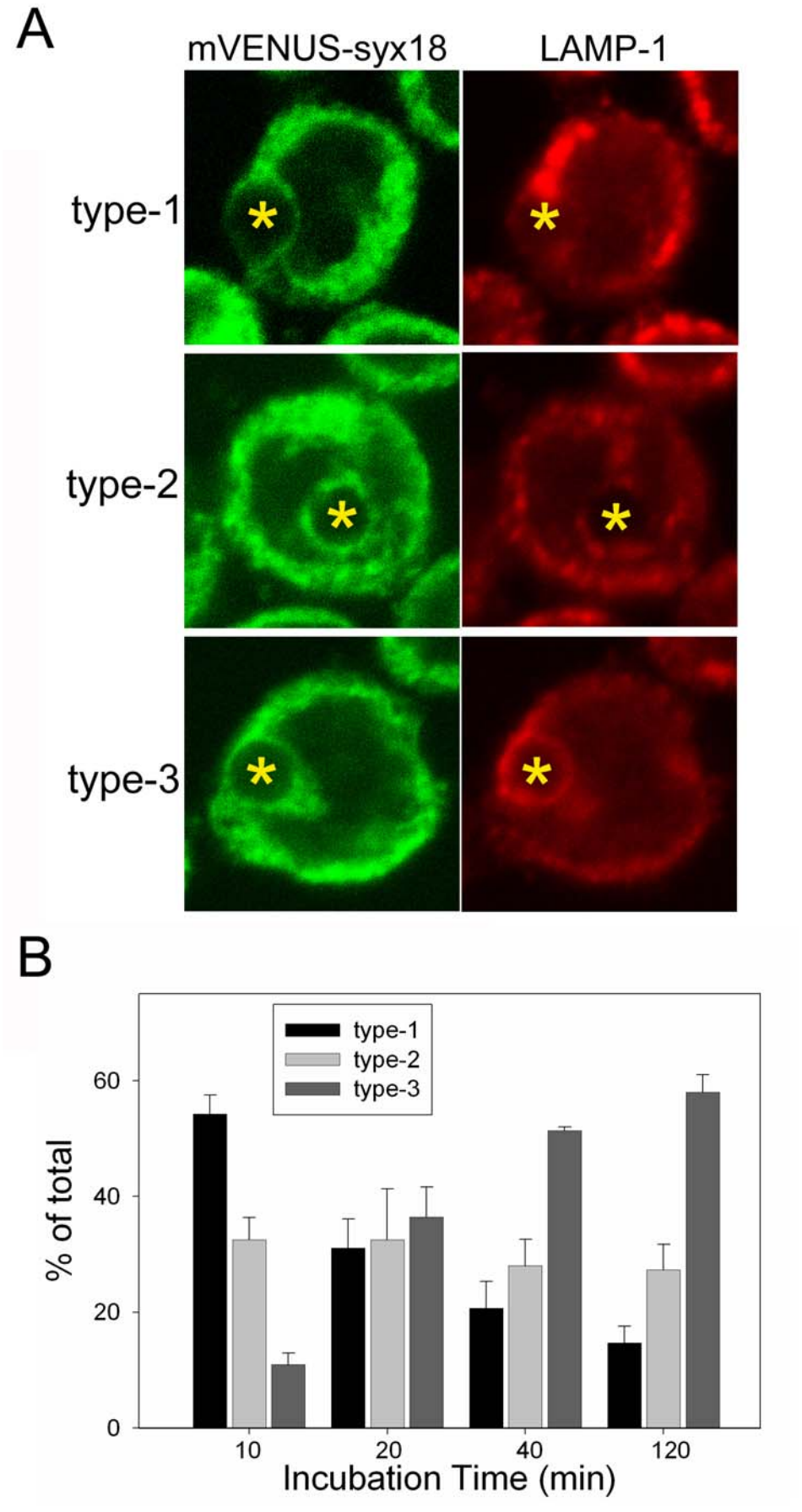

Supplementary Figure S2. Hatsuzawa *et al.*

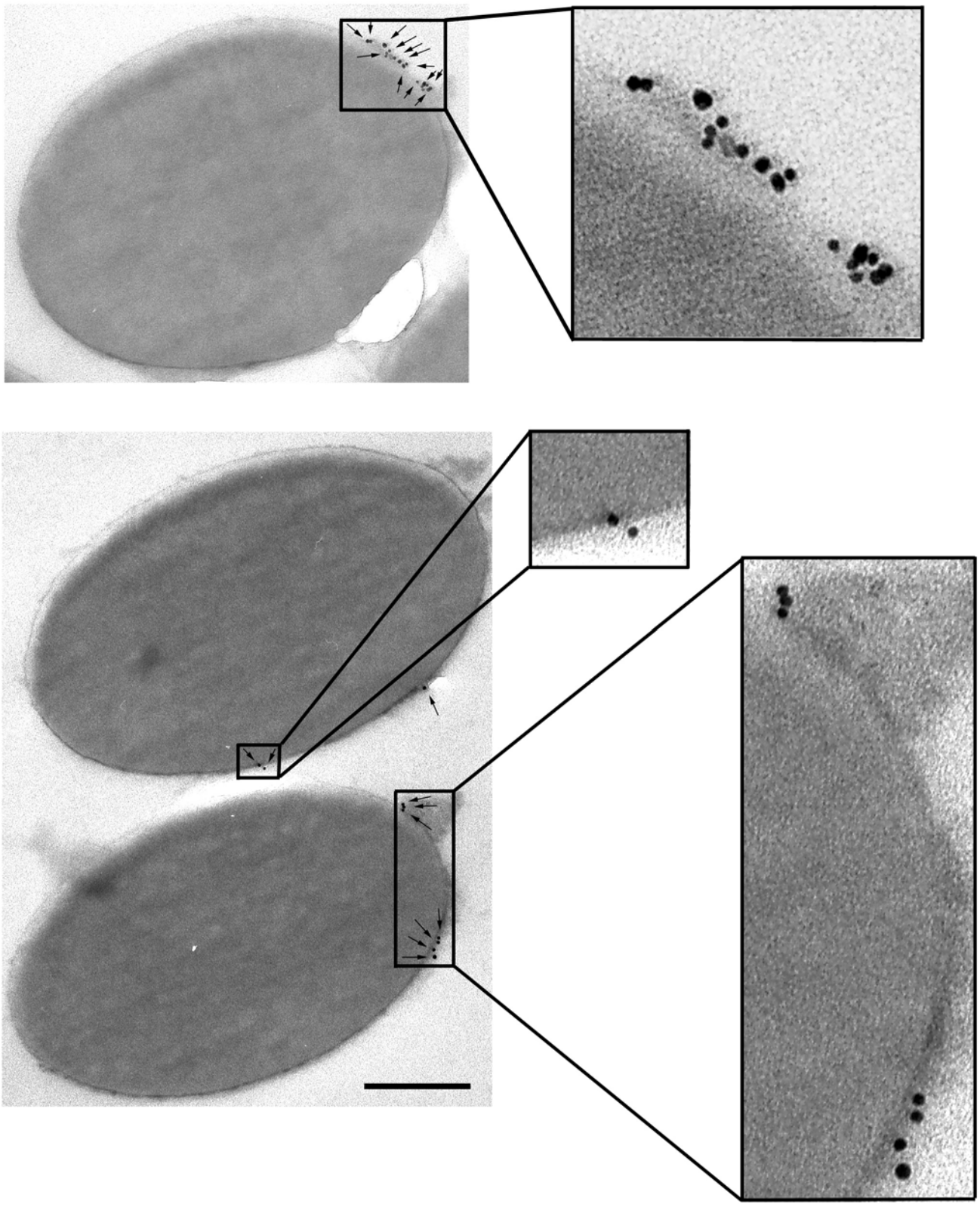

Supplementary Figure S3. Hatsuzawa *et al.*

B

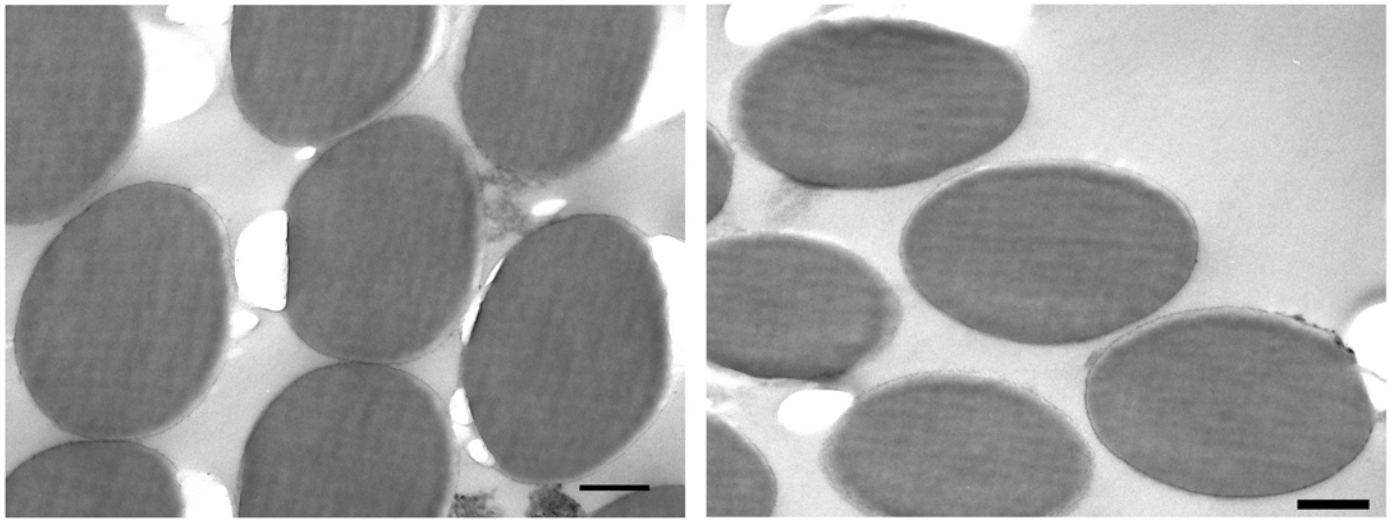

C

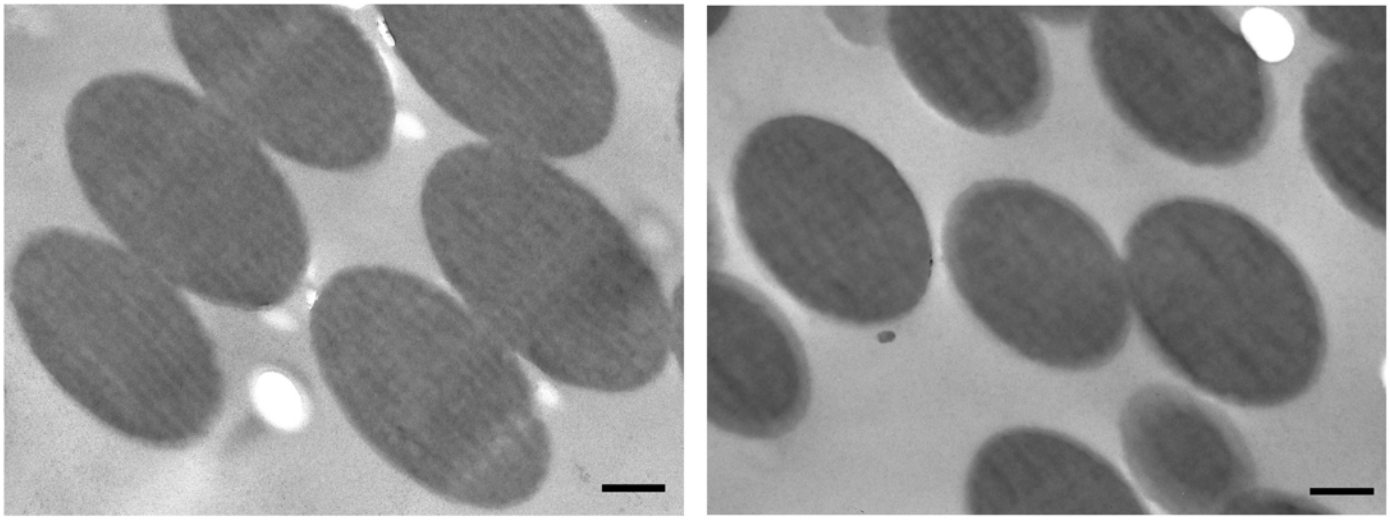

Supplementary Figure S3. Hatsuzawa *et al.*

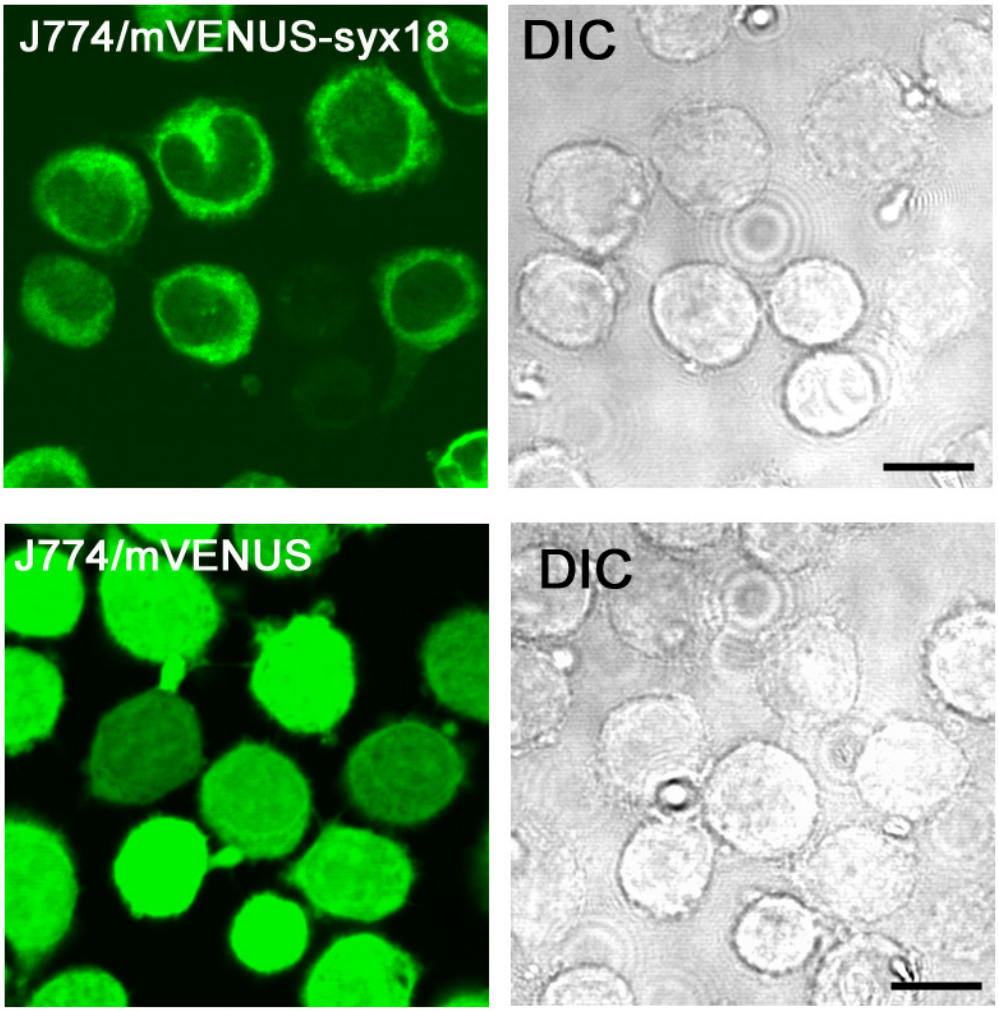

Supplementary Figure S4. Hatsuzawa *et al.*

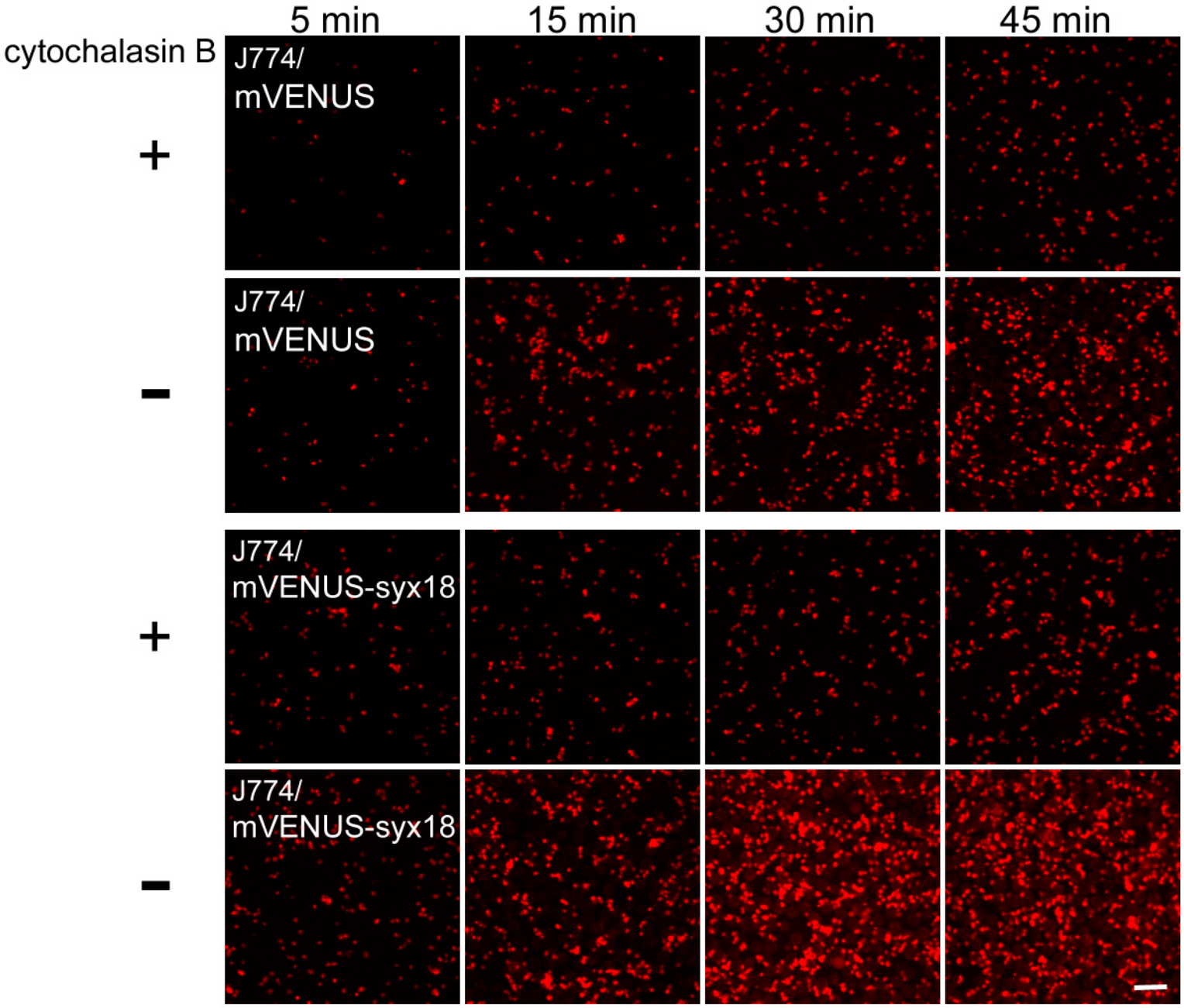

Supplementary Figure S5. Hatsuzawa *et al.*